Available online at www.CivileJournal.org

Civil Engineering Journal

(E-ISSN: 2476-3055; ISSN: 2676-6957)

Vol. 8, No. 11, November, 2022

Optimal Compressive Strength of RHA Ultra-High-Performance Lightweight Concrete (UHPLC) and Its Environmental Performance Using Life Cycle Assessment

Kennedy C. Onyelowe [1], Ahmed M. Ebid [2*], Hisham A. Mahdi [2], Ariel Riofrio [3], Danial Rezazadeh Eidgahee [4], Haci Baykara [3], Atefeh Soleymani [5], Denise-Penelope N. Kontoni [6], Jamshid Shakeri [7], Hashem Jahangir [8]

[1] Department of Civil Engineering, Michael Okpara University of Agriculture Umudike, 440109, Umuahia, Nigeria.

[2] Faculty of Engineering and Technology, Future University in Egypt, New Cairo 11865, Egypt.

[3] Escuela Superior Politécnica del Litoral, ESPOL, Campus Gustavo Galindo, Guayaquil, Ecuador.

[4] Faculty of Civil Engineering, Semnan University, Semnan, Iran.

[5] Department of Civil Engineering, Shahid Bahonar University of Kerman, Kerman, Iran.

[6] Department of Civil Engineering, School of Engineering, University of the Peloponnese, GR-26335 Patras, Greece.

[7] Department of Mining Engineering, Faculty of Engineering, University of Kurdistan, Sanandaj, Iran.

[8] Department of Civil Engineering, University of Birjand, Birjand, Iran.

Received 20 July 2022; Revised 01 October 2022; Accepted 12 October 2022; Published 01 November 2022

Abstract

Frequent laboratory needs during the production of concrete for infrastructure development purposes are a factor of serious concern for sustainable development. In order to overcome this trend, an intelligent forecast of the concrete properties based on multiple data points collected from various concrete mixes produced and cured under different conditions is adopted. It is equally important to consider the impact of the concrete components in this attempt to take care of the environmental risks involved in this production. In this work, 192 mixes of an ultra-high-performance lightweight concrete (UHPLC) were collected from literature representing different mixes cured under different periods and laboratory conditions. These mix proportions constitute measured variables, which are curing age (A), cement content (C), fine aggregate (FAg), plasticizer (PL), and rice husk ash (RHA). The studied concrete property was the unconfined compressive strength (Fc). This exercise was necessary to reduce multiple dependence on laboratory examinations by proposing concrete strength equations. First, the life cycle assessment evaluation was conducted on the rice husk ash-based UHPLC, and the results from the 192 mixes show that the C-783 mix (87 kg/m^3 RHA) has the highest score on the environmental performance evaluation, while C-300 (75 kg/m^3 RHA) with life cycle indices of 289.85 kg CO_{2eq}. Global warming potential (GWP), 0.66 kg SO_{2eq}. Terrestrial acidification and 5.77 m^3 water consumption was selected to be the optimal choice due to its good profile in the LCA and the Fc associated with the mix. Second, intelligent predictions were conducted by using six algorithms (ANN-BP), (ANN-GRG), (ANN-GA), (GP), (EPR), and (GMDH-Combi). The results show that (ANN-BP) with performance indices of R; 0.989, R^2; 0.979, mean square error (MSE); 2252.55, root mean squared error (RMSE); 42.46 MPa and mean absolute percentage error (MAPE); 4.95% outclassed the other five techniques and is selected as the decisive model. However, it also compared well and outclassed previous models, which had used gene expression programming (GEP) and random forest regression (RFR) and achieved R^2 of 0.96 and 0.91, respectively.

Keywords: Lightweight Concrete; Sustainable Construction; Environmental Impact; Life Cycle Impact Assessment; Green Concrete.

---

* Corresponding author: ahmed.abdelkhaleq@fue.edu.eg

http://dx.doi.org/10.28991/CEJ-2022-08-11-03

© 2022 by the authors. Licensee C.E.J, Tehran, Iran. This article is an open access article distributed under the terms and conditions of the Creative Commons Attribution (CC-BY) license (http://creativecommons.org/licenses/by/4.0/).

1. Introduction

Concrete is the most commonly used building material in the construction sector due to its many advantages, including being readily available in all parts of the world, being inexpensive, and having good mechanical qualities [1–4]. The building sector consumes the majority of raw materials [5]. Cement is utilized as a binder ingredient in concrete and is responsible for the construction industry's carbon emissions [6, 7]. In other words, concrete manufacturing has a significant environmental impact, and environmental issues in the building sector are well known [8–11].

Researchers all across the world are working to reduce the amount of cement used in concrete in order to enhance its engineering characteristics. To partially decrease the quantity of cement in concrete, the various available alternate binding materials are blast furnace slag (BFS) [12], fly ash [13, 14], rice husk ash [15], plastic powder [16], bagasse ash [16], etc. The supplementary materials are sustainable for nature and also lower the overall cost of construction [17]. However, these novel materials must be assessed in terms of cost, quality, performance, and environmental implications. To attain this aim, a well-known method called life cycle assessment (LCA) method may be used to study the impact of a material or methodology on the environment [18, 19]. LCA permits us to balance both the energy and material usage while quantifying total environmental implications [20, 21]. LCA is a potentially viable method for evaluating the environmental performance of construction materials [22–27].

Due to developments in mechanical and durability qualities with compressive strengths greater than 150 MPa, Ultra High-Performance Concrete (UHPC) is now considered the most recent breakthrough in the world of concrete technology [28–30]. Mineral admixtures, such as rice husk ash, are natural pozzolanic materials with high amorphous silica content and highly fine texture, which can be a UHPC ingredient like silica fume, but in developing nations the cost of silica fume is very high [31–36]. It is now critical for researchers and construction workers to identify an alternate material with equivalent properties to use in the manufacturing of UHPC. Silica fume has comparatively large particle sizes that are beyond 10 µm and is also extremely tough to break due to its strong inter-atomic interactions (Van der Waal's forces), even in the existence of moisture. In terms of technical and environmental impact evaluation at a cheaper cost, RHA can be an excellent option, and it can significantly improve its mechanical and durability qualities [37–39]. RHA has almost similar chemical composition to SF [40], but the difference in particle size makes it particularly effective in the hydration development and improving the microstructure of the paste of cement [41, 42].

Rice husk (RH) is the hard external layer of paddy rice that separates rice grains during the milling process. It accounts for roughly 20–30% of the weight of yearly rice output, which was anticipated to reach 760 million tons in 2017 and is probable to grow by 2050. Nearly 150 million tons (18–25%) of milled material are disposed of in landfills or waterways, posing environmental concerns like pollution [43, 44]. During the burning process, it loses approximately 80% of its weight and changes to RHA since it comprises 20% inorganic and 80% organic components [45]. It has been proven to be a natural supply of silica as well as having faults that may be addressed with citric acid to do the purification before burning, so contributing to the production of sustainable concrete [46]. With a high silica content, high specific area, an amorphous silica crystallization phase, high pozzolanic activity, and a porous microstructure, the solid residual RHA has attracted a lot of interest due to its availability and affordability. As a result, it has the potential to be a useful supplemental cementitious material [47–51]. Using RHA instead of SF in concrete manufacturing has enhanced the concrete's characteristics while also reducing pollution and expense. This RHA can increase the hydration and mechanical characteristics of the concrete, in addition to its high durability, chemical attack resistance, and freeze-thaw resistance, according to a group of Chinese researchers [52].

Van Tuan et al. [53] investigated the feasibility of employing RHA to manufacture the UHPC. The consequences demonstrated that the mechanical strength of UHPC containing RHA may exceed 150 MPa under typical curing conditions. The fact that RHA had a greater influence on the enhancement of compressive strength in UHPC than SF is noteworthy. Furthermore, the sample containing the ternary cement mix with 10% SF and 10% RHA had a higher mechanical strength than the reference sample without SF or RHA. This combination proved to be the most effective solution for obtaining the maximum synergy. The goal of the Lu et al. study [54] was to use a mathematical technique to build a revolutionary lightweight UHPC (L-UHPC) with low density and great performance. The L-UHPC mix design included two lightweight ingredients (expanded shale aggregates and micro-sized glass microspheres). The L-UHPC was created using numerical optimization using a central composite design, which proved to be a successful strategy. The developed L-UHPC had functional and durability attributes that were equivalent to or even higher properties as compared to high-performance cement mortar (HPCM) and normal-weight UHPC.

Various studies on the LCA of cement and concrete have been conducted. Heede & Belie [55] shows the comparison between conventional concrete and sustainable concrete study the impact on the environmental. Authors used the "damage-oriented IMPACT 2002plus method" and "problem-oriented CML 2002" technique to assess the environmental consequences. Their findings showed that green concrete (concrete manufactured from furnace slag) pollutes the environment less than concrete created from Portland cement. According to the Liu et al. [56], environmental LCA of reactive powder concrete and conventional concrete on a dam building plan in China, RFC concrete had 64% and 55% lower greenhouse gas emissions and energy usage, respectively, than conventional concrete. The quantity of carbon dioxide was decreases mainly in four stages such as material production, transportation, construction, and operation and maintenance with values 72%, 25%, 51% and 15.6%, respectively.

Using SimaPro8 software, Cheung & Tait [57] investigated the cradle-to-gate (LCA) of concrete contains 100% cement (first case), 35% FA and 65% cement (2nd case), and 70% slag of the furnace and 30% cement (3rd case),and environmental impressions were evaluated using Eco-points 97 and Eco-indicator 99 methods. In comparison to standard concrete, their findings revealed that the 62% and 32% of carbon emission reduced in the second and third type of the concrete, respectively.

Anastasiou & Papayianni conducted a comparative LCA for six unique concrete pavements in their work [58]. Pozzolanic Portland cement (PPC), mixed-type binder with PC and FA and a novel hydraulic road binder were used binder materials in the road pavements. Adding to that, two distinct aggregates such as; steel slag and crushed limestone, were used in the comparative LCA. For the LCA, the construction, usage, and maintenance, as well as end-of-life recycling, were all taken into account during a 40-year period. The findings revealed that the concrete pavements with a large proportion of substitute materials can considerably lower CO2 emissions and so improve their environmental footprint when compared to standard concrete pavements.

The impact of recycled aggregates and FA in concrete was explored by Kurad et al. [59]. To examine the potential for global warming of concrete, the CML approach was used to analyze environmental implications. There were three mix groups: 100% fine RCA, 50% fine RCA and 0% fine RCA. The average global warming potential (GWP) was reduced by 0.91%, 0.02%, and 0.91% per kg, respectively, and it was further reduced by 2% by applying a 1% superplasticizer. Figure 1 presents the multiple benefits of RHA in concrete.

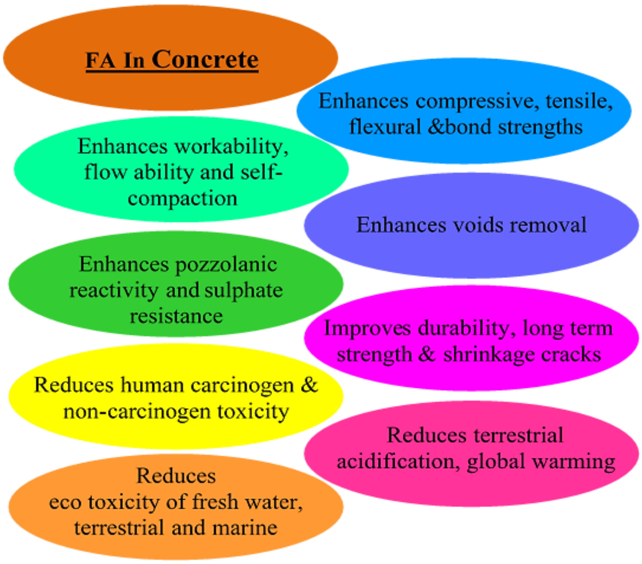

Figure 1. Benefit of rice husk ash to the structural and environmental behavior of UHPLC concrete

In this paper, the life cycle assessment of RHA in UHPLC has been evaluated to determine its potential contribution to global warming potential under carbon footprint considerations, terrestrial acidification and water potential. Also, the compressive strength of the studied concrete has been predicted by using intelligent techniques, which include three hybrids of ANN, genetic programming, evolutionary polynomial regression and combinatorial group method of data handling. In the LCA evaluation and prediction exercises, concrete age, cement content, rice husk ash, water, super plasticizer, and fine aggregates were used as the input's variables from a data of 192 mixes collected from literature.

2. Methodology

2.1. Ultra-High-Performance Concrete Mix Data Collection and Statistical Analysis

Extensive literature search and data curation were the methods of data collection adopted in this research work. A concrete mix database of 192 mixes were collected from a previous research study by Iftikhar et al. [60]. The records were collected from different mixes of experimentally tested concrete mixtures with different components' ratios, cured under different conditions. Each record contains the following data: concrete age (A) days, cement content (C) kg/m^3, rice husk ash content (RHA) kg/m^3, water content (W) kg/m^3, super plasticizer content (PL) kg/m^3, fine aggregates content (FAg) kg/m^3, cylinder compressive strength of concrete (Fc) MPa. The collected records were divided into training set (150 records) and validation set (42 records). In Tables 1 and 2, the statistical characteristics and the Pearson correlation matrix of the collected data for the studied variables are summarized and Figure 2 shows the histograms for both inputs and outputs.

Table 1. Statistical analysis of studied concrete mix variables

	Minimum	Maximum	Range	Mean	S.D.	Var.	Skewness	Kurtosis
A	1.00	90.00	89.00	34.57	33.52	1123.6	0.75	-1.02
C	249.0	783.00	534.0	409.06	105.46	11121	1.55	3.66
RHA	0.00	171.00	171.0	62.33	41.54	1725.7	0.44	0.08
W	120.00	238.00	118.0	193.56	31.90	1017.3	-0.42	-0.75
PL	0.00	11.30	11.30	3.34	3.52	12.40	0.70	-0.81
FAg	1040.0	1970.0	930.0	1621.51	267.77	71702	-0.74	-0.27
Fc	16.00	104.00	88.00	48.21	17.50	306.29	0.83	0.73

Table 2. Pearson correlation matrix of the studied concrete variables

	A	C	RHA	W	PL	FAg	Fc
A	1.00						
C	-0.11	1.00					
RHA	-0.03	-0.22	1.00				
W	0.01	0.08	0.14	1.00			
PL	0.00	0.25	-0.02	0.27	1.00		
FAg	-0.06	-0.24	-0.14	-0.55	-0.21	1.00	
Fc	0.49	0.37	-0.02	-0.24	0.30	0.15	1.00

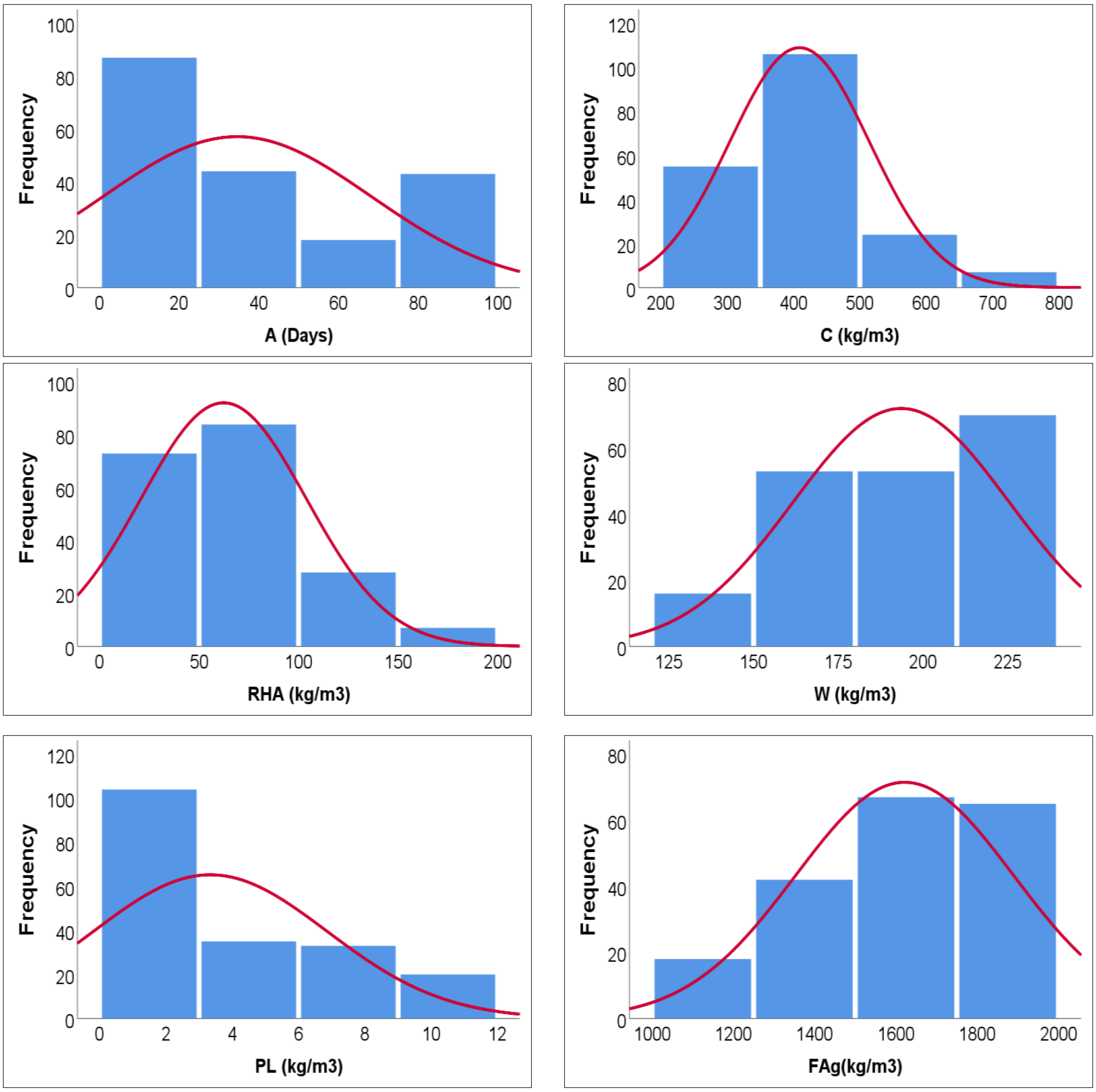

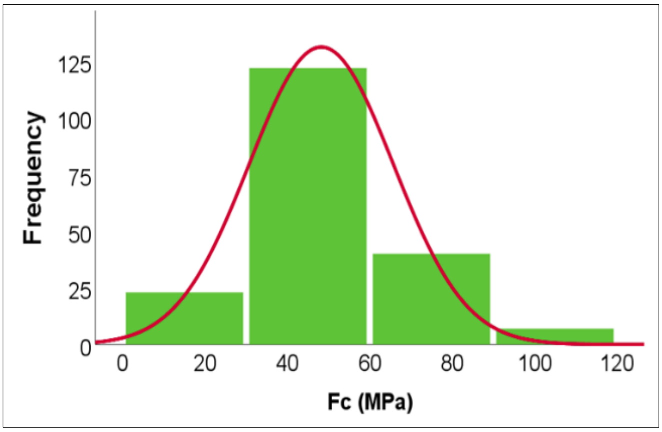

Figure 2. Distribution histograms for inputs (in blue) and outputs (in green)

2.2. Research Program Plan

Life cycle impact assessment evaluation was carried out on the rice husk ash (RHA) ultra-high performance lightweight concrete (UHPLC) to determine the global warming potential (GWP) (carbon footprint), terrestrial acidification (acid potential), and the water potential of the multiple concrete mixes produced under different laboratory conditions and cured at different days. Furthermore, five different soft computing techniques were deployed to forecast the compressive strength (Fc) of ultra-high-performance lightweight concrete using the gathered dataset. The implemented techniques are the hybrids of artificial neural network, which include ANN-BP, ANN-GRG and ANN-GA, genetic programming (GP) and the evolutionary polynomial regression (EPR). All these intelligent techniques were used to predict the compressive strength of concrete at certain age (Fc, MPa) using concrete curing age (A) days, cement content (C) kg/m3, rice husk ash content (RHA) kg/m^3, water content (W) kg/m^3, super plasticizer content (PL) kg/m^3 and fine aggregates content (FAg) kg/$m^{3.}$

Each deployed intelligent method is based on different approaches, which mimic the human brain for the working of the ANN, optimization of mathematical regression for EPR and simulating evolution of natural creatures for GP. However, for all techniques, their accuracies were estimated on basis of mean absolute percentage error (MAPE), mean squared error (MSE), root of mean of squared errors (RMSE), correlation coefficient (R) and determination coefficient (R^2). The next sections present the results of the environmental impact assessment and each intelligent method utilized and its accuracy metrics.

2.3. Life Cycle Assessment: Goal, Scope and Functional Unit

Environmental performance of materials and circular economy are considered two critical factors when developing any kind of new material. The normative ISO 14040 [61] analyzes the effect on the environment of energy use and materials, among other parameters taking a life cycle perspective into account. A life cycle assessment (LCA) allows for the evaluation of the environmental burden and optimization opportunities without shifting it from one step of the life cycle to another. The main goal of the LCA is to evaluate and analyze the environmental impact of adding rice husk ash to a cement matrix. A more complex life cycle assessment study has been performed based on varying a large number of data compositions from the 192 mixes of UHPLC. The functional unit established is 1 m^3 of concrete mix using rice husk ash (RHA). The scope of this study covers the extraction and use of raw materials such as cement, superplasticizer, fine aggregates, and RHA. The system boundary represents the scheme of the scope of the LCA study as presented in Figure 3.

The concrete mixes considered for the LCA in this study were identified using cement composition. If two or more concrete mixtures have the same amount of Ordinary Portland cement (OPC), then the superplasticizer is used as an identifier. For instance, C-425-SP-5 identifies a concrete mix that uses 425 kg of Portland cement and 5 kg of superplasticizer.

2.4. Life Cycle Assessment: Inventory and Method

The data was modelled using the EcoInvent Database 3.2 [62] for materials such as Portland cement, fine aggregates, superplasticizer, electricity, water, and creating the inventory for the rice husk ash (RHA) as a waste from the cogeneration of electricity. The inventory accounts for materials, energy, and transportation that can be converted directly to impact indicators. In this study, ReCiPe Midpoint H [63] method was used for data conversion to impact categories. This method allows for a global approach while maintaining a hierarchy perspective at the midpoint level. This means a balanced environmental performance assessment for the cradle-to-gate evaluation of the cementitious material.

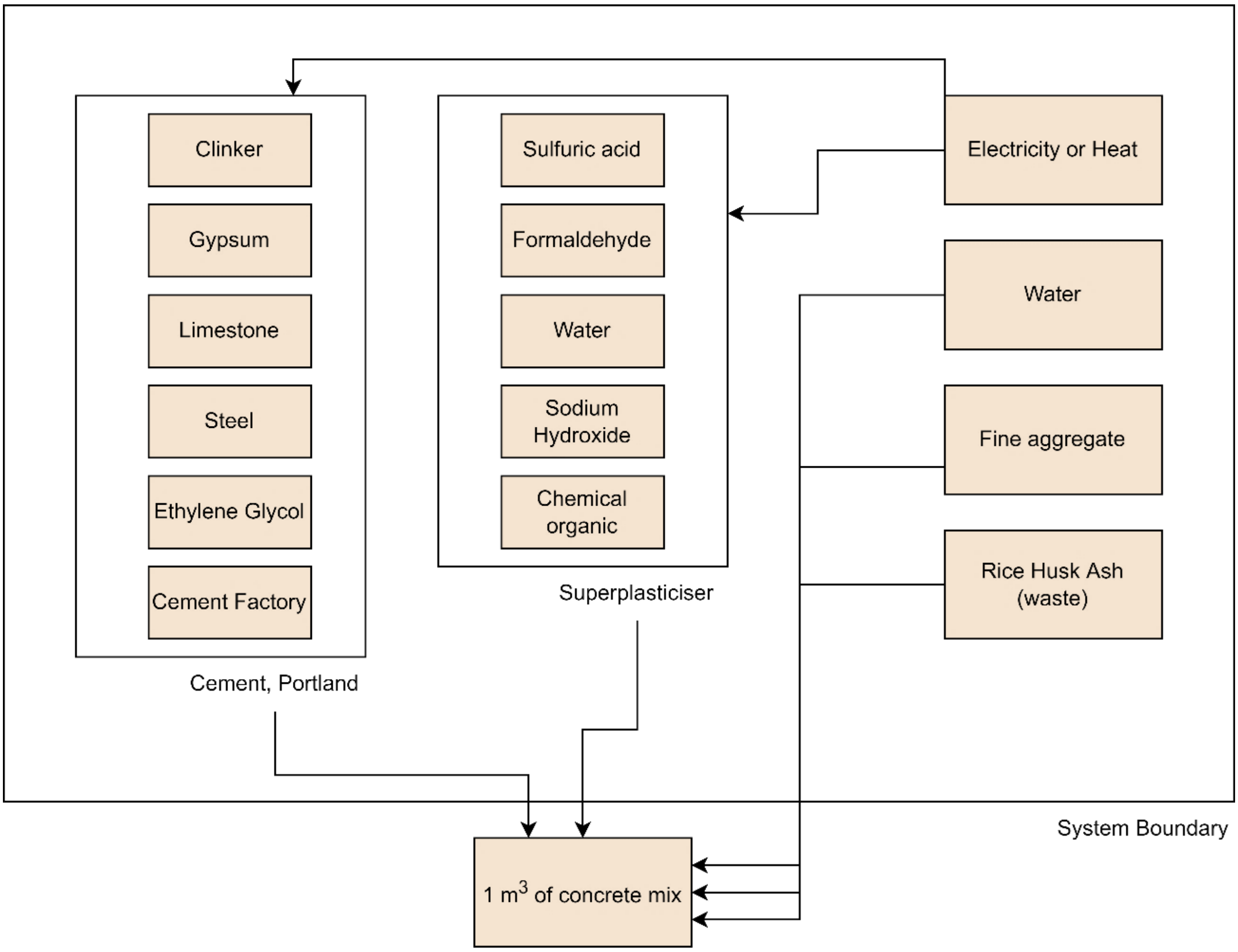

Figure 3. System boundary for the production of 1 m3 of cement mix using RHA

3. Results and Discussions

3.1. Environmental Impact Assessment of RHA in UHPLC

3.1.1. Summary Remarks

The life cycle analysis was performed on the different mixes with varying RHA as an alternative cementitious material. Three main categories were evaluated in the assessment: global warming/carbon footprint, terrestrial acidification/acid potential, and water consumption/water footprint. Table 3 presents the results from the different concrete mixes analysed for the specified categories. Results show a direct relation in the use of cement in the concrete with the increase of certain environmental indicators such as global warming. The importance of including rice husk ash as a silicate source will result in the enhancement of the concrete matrixes' environmental profile.

3.1.2. Carbon Footprint

Normalizing data in an LCA study helps the reader understand and compare the results appropriately. For this purpose, the normalized LCA results are also given for comparison between evaluated concrete mixes in the current study. Figure 4 shows the normalized environmental impacts for the concrete mixes analysed. The carbon footprint increases with the addition of cement to the concrete mix. The C-783 mix is the most pollutant one in terms of carbon dioxide emissions. On the other side, C-249 and C-300 concrete samples emit lower CO2. The line of tendency shows an increase because of the use of cement, but variations can be seen because of the inclusion of superplasticizer without RHA addition. The OPC concrete has a global warming potential of 386 kg CO2 eq., which is 33% more carbon dioxide emitted than the C-300 mix [64]. Asadollahfardi et al. [64] analysed geopolymer concrete, micro, and nano-silica concrete. The results showed that the geopolymer concrete has roughly the same carbon footprint as C-300 but a higher impact on the silica mixes. Different studies in the literature report an average impact of 350-400 kg of CO2 emissions for the production of similar concrete samples [64–66].

Table 3. LCA results for the different concrete mixes analyzed

Impact Category	Global Warming	Terrestrial acidification	Water consumption	Impact Category	Global Warming	Terrestrial acidification	Water consumption
Code/Unit	**kg CO_2 eq**	**kg SO_2 eq**	**(m^3)**	**Code/Unit**	**kg CO_2 eq**	**kg SO_2 eq**	**(m^3)**
C-249	289.42	0.85	8.35	C-383-SP-0.3	389.01	0.74	4.98
C-268	301.51	0.81	7.64	C-391	370.10	0.67	4.37
C-287	313.61	0.78	6.94	C-400-SP-3.7	451.79	1.20	10.06
C-300	289.85	0.66	5.77	C-400-SP-6.22	383.21	0.88	6.83
C-306	325.71	0.74	6.23	C-400-SP-7.36	384.51	0.88	6.86
C-315	354.74	0.86	6.93	C-405	473.37	0.91	5.56
C-318	300.58	0.63	5.15	C-416	578.68	1.05	5.73
C-326	338.44	0.70	5.49	C-420	564.19	0.86	3.49
C-327	335.70	0.71	4.86	C-425-SP-5	400.74	0.84	6.02
C-337.5	311.31	0.60	4.53	C-425-SP-6.4	402.39	0.85	6.07
C-337.5-SP-8.4375	419.81	0.97	7.40	C-427	598.31	1.25	8.01
C-345	350.54	0.67	4.78	C-427.5	492.16	0.88	4.79
C-356	322.04	0.57	3.91	C-450	509.16	0.84	3.91
C-357	349.64	0.73	5.56	C-457	481.94	1.08	7.80
C-360	437.93	0.95	6.87	C-481	656.15	1.20	6.20
C-364	362.64	0.63	4.08	C-495-SP-5.8	451.92	0.86	5.39
C-367	530.92	0.97	5.56	C-495-SP-6.8	453.21	0.87	5.42
C-370	537.02	1.13	7.47	C-500-SP-5.5	433.68	0.70	3.49
C-375	332.78	0.54	3.29	C-500-SP-6.5	434.95	0.71	3.52
C-378	362.28	0.69	4.79	C-514	512.37	0.95	5.61
C-382	455.32	0.93	6.16	C-571	542.72	0.84	3.48
C-383	374.74	0.60	3.32	C-783	780.65	1.43	7.03

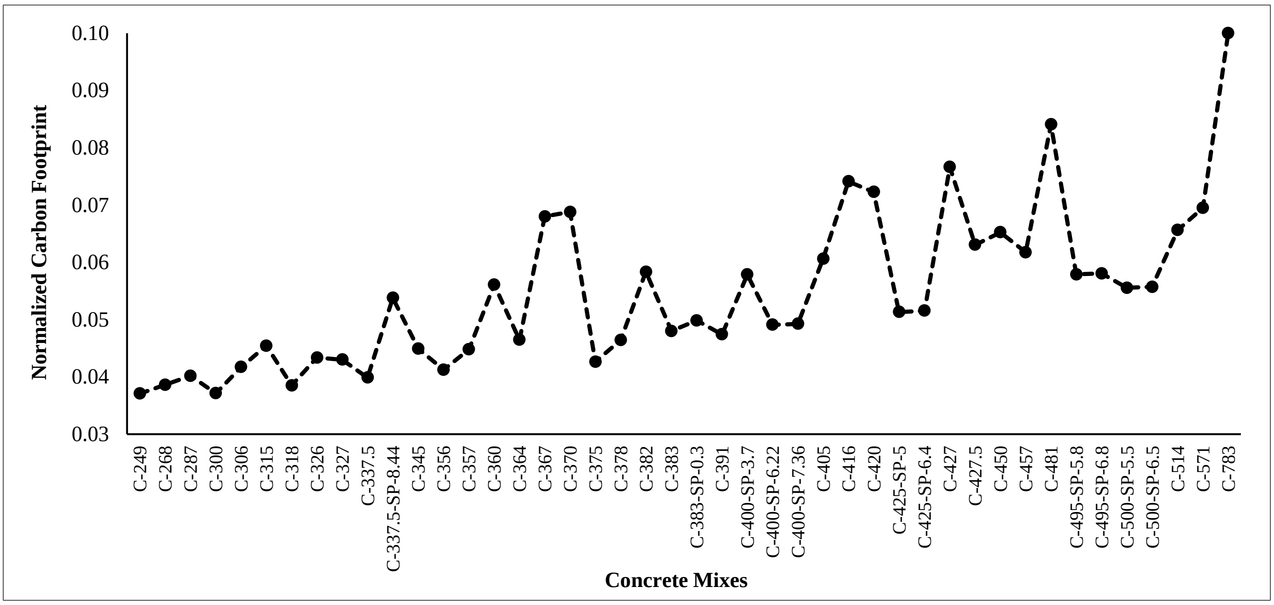

Figure 4. The normalized carbon footprint of the different concrete mixes

3.1.3. Acid Potential

The acid potential can be seen in Figure 5. As seen in the figure, normalized results were given for this impact indicator for an easier comparison. Once again, the C-783 concrete mix shows a higher impact in this category. This reinforces the significance of the Portland cement on the overall impact of the concretes to be studied. The lowest impact in this category was found to be the mix C-375. However, the concrete C-300 has performed well in the terrestrial acidification category. In the same sense, literature [64, 66, 67] shows that pure OPC has an acidification potential 27% higher than the C-300 mix. Even though it is not the optimal mix for this indicator, it has a better environmental performance than pure OPC.

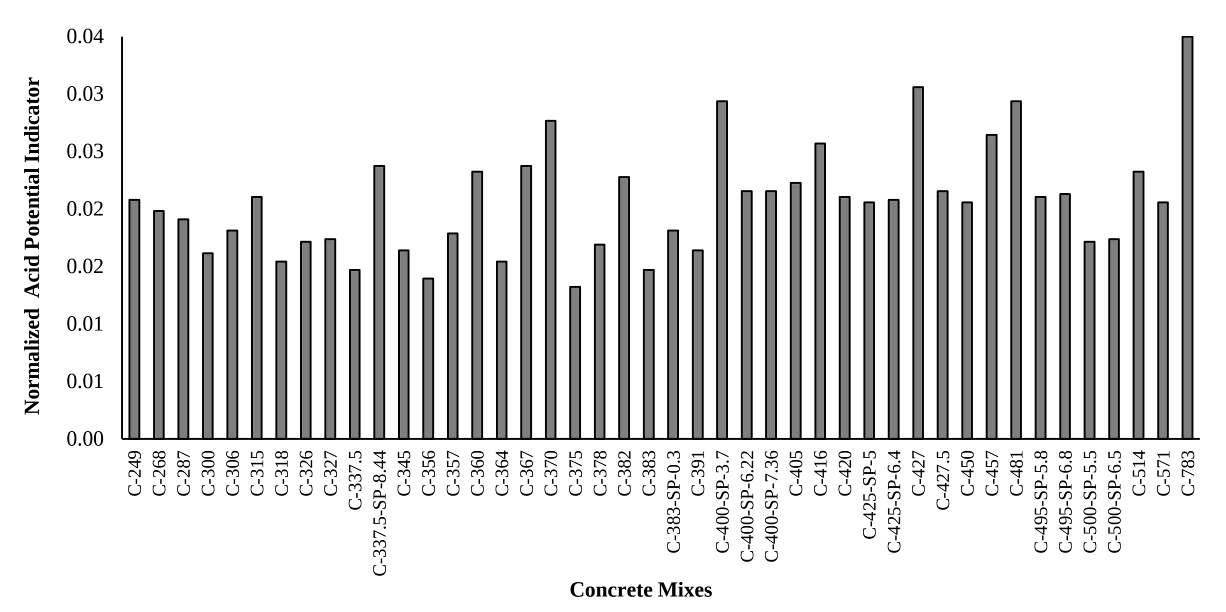

Figure 5. Normalized results for the acid potential indicator

3.1.4. Water Footprint

Another critical category to be evaluated is the water footprint because water supply shortages occur worldwide. Thus, the demand for water from the cement and concrete industry can be significant. Figure 6 shows variation in the results for water consumption. As seen in the figure, the amount of water required in all the processes to achieve the preparation of the C-391 concrete sample is the highest. This is related to the higher content of water added to the mixture plus the consumed water by the elaboration of the other materials like the plasticizer and cement. The concrete C-300 has a balanced impact towards the middle of the data evaluated.

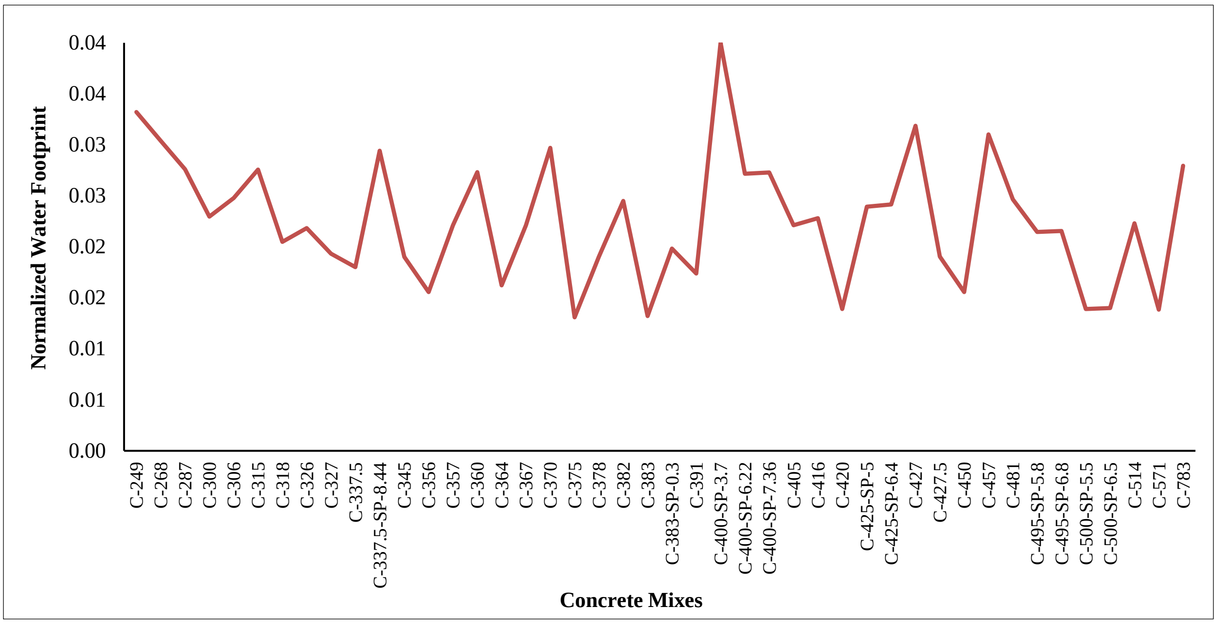

Figure 6. The water footprint of the different concrete mixes

3.1.5. Process Contribution

The C-300 matrix was analysed to assess the contribution of each of the materials needed for the concrete because it performed well under the LCA methodology. The first parameter is that this concrete mix does not require a superplasticizer, which would add significant value to the environmental categories discussed earlier. In addition, the OPC is the major contributor (~56%) in almost every category of the 18-impact indicators analysed with the ReCiPe Midpoint H [63] method. The rice husk ash has the majority of the contribution to ozone depletion (67%), marine eutrophication (88%), and freshwater eco-toxicity (55%). Fine aggregates have lesser contributions except for terrestrial eco-toxicity and water consumption, with 48 and 45%, respectively as shown in Figure 7. One study showed similar behaviour for the contribution of concrete towards environmental impact indicators, reporting the OPC as one of the significant contributors [68].

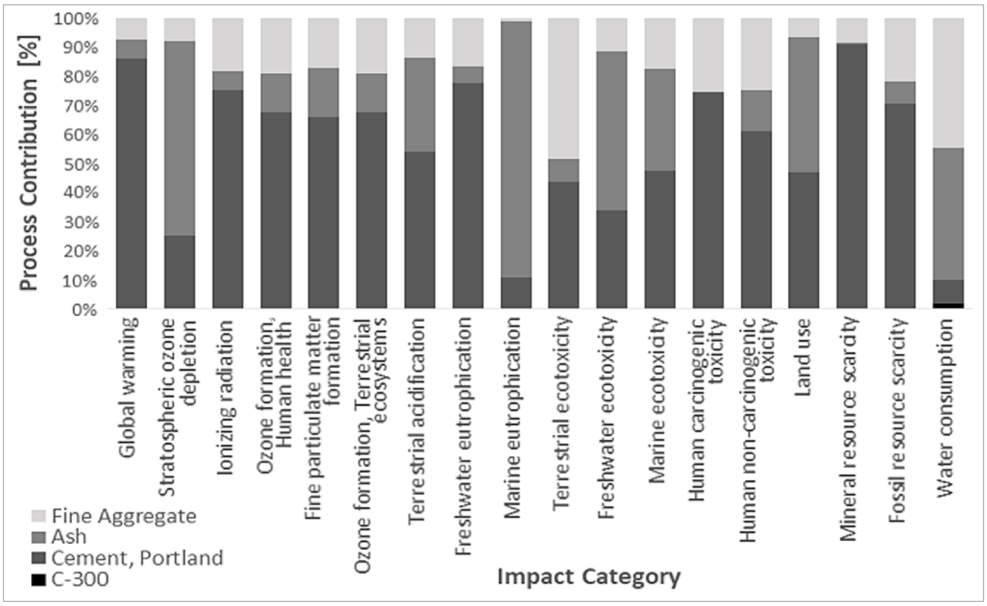

Figure 7. Process contribution for the C-300 concrete mix

3.2. AI Predictions for the UHPLC Compressive Strength (Fc)

3.2.1. ANN Prediction

Three models were developed using (ANN) technique. All the models have the same layout (6:5:1), standardization method (Var/S.D) and activation function (Hyper Tan). However, each model utilized different training algorithm as follows: the traditional "back propagation (BP)" algorithm, the well-known mathematical algorithm "gradually reduced gradient (GRG)", the famous (AI) optimization technique "genetic algorithm (GA)". These three developed models were used to predict (Fc) values. The used networks layout is illustrated in Figure 8 while the weight matrixes of each model are showed in Tables 4 to 6. The average errors of total dataset are 5.3MPa, 5.8MPa and 7.3MPa and the R^2 values are 0.977, 0.973 and 0.957 respectively. These outcomes compare well with a previous study [60] which utilized GEP and RFR and achieved R2 of 0.96 and 0.91 with ANN-BP and –GRG showing better outcome and ANN-GA at par with GEP of the previous study.

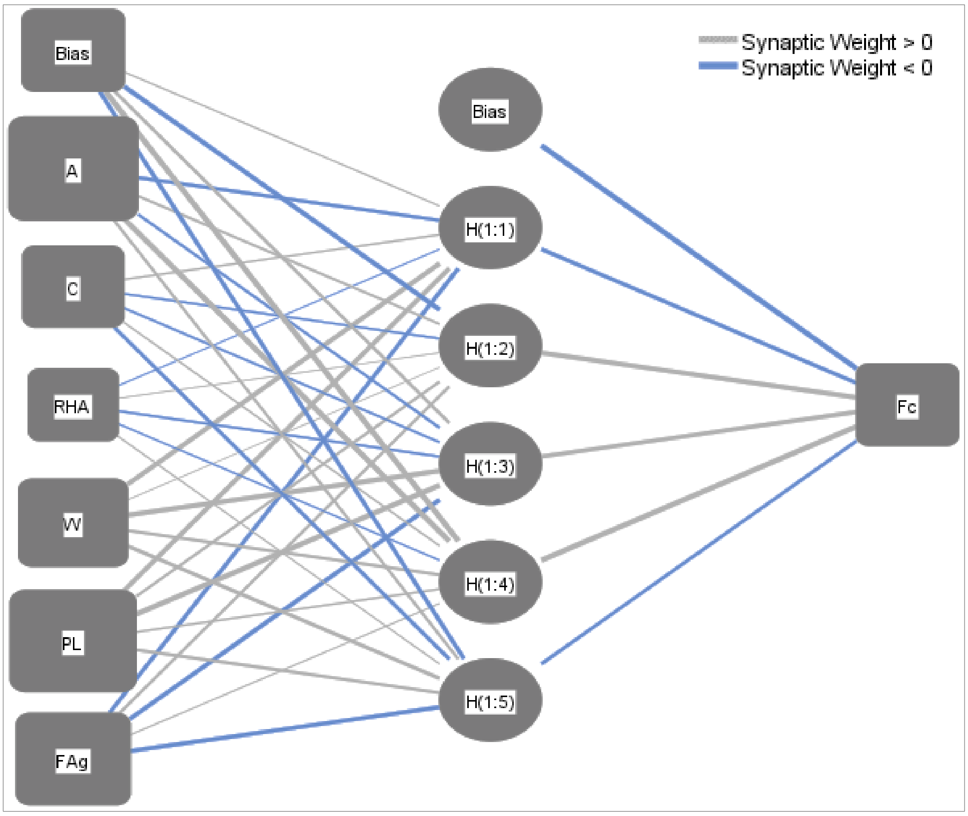

Figure 8. Layout for the developed ANN models

Table 4. Weights matrix for the developed ANN –BP model

		Hidden Layer 1					
		H(1:1)	**H(1:2)**	**H(1:3)**	**H(1:4)**	**H(1:5)**	
Input Layer	(Bias)	-0.034	0.385	-0.170	0.245	-9.370	
	A	0.389	-0.313	-0.063	0.052	-8.590	
	C	-1.249	0.239	-0.022	0.153	-0.151	
	RHA	-1.078	0.193	0.122	0.562	0.026	
	W	1.972	0.339	0.222	0.608	-0.381	
	PL	4.192	-0.414	-0.061	-0.058	-0.237	
	FAg	-2.260	1.312	0.182	0.364	-0.210	
		Hidden Layer 1					
		H(1:1)	**H(1:2)**	**H(1:3)**	**H(1:4)**	**H(1:5)**	**(Bias)**
Output Layer	Fc	0.924	1.554	-4.221	1.361	-3.722	-4.977

Table 5. Weights matrix for the developed ANN –GRG model

		Hidden Layer 1					
		H(1:1)	**H(1:2)**	**H(1:3)**	**H(1:4)**	**H(1:5)**	
Input Layer	(Bias)	8.651	-0.281	-7.089	0.162	0.509	
	A	7.573	-0.047	0.141	-0.011	-0.153	
	C	0.155	0.292	2.107	-0.240	-0.649	
	RHA	-0.035	-0.535	0.754	0.433	-0.191	
	W	0.355	-0.203	3.311	0.266	-0.277	
	PL	0.219	0.232	2.481	-0.375	0.654	
	FAg	0.171	-0.188	6.573	0.048	0.338	
		Hidden Layer 1					
		H(1:1)	**H(1:2)**	**H(1:3)**	**H(1:4)**	**H(1:5)**	**(Bias)**
Output Layer	Fc	6.337	-1.971	4.503	-2.222	-0.582	-1.987

Table 6. Weights matrix for the developed ANN –GA model

		Hidden Layer 1					
		H(1:1)	**H(1:2)**	**H(1:3)**	**H(1:4)**	**H(1:5)**	
Input Layer	(Bias)	0.054	-1.093	0.453	5.565	-0.872	
	A	-0.541	0.181	-0.193	4.852	0.215	
	C	0.083	-0.128	-0.147	0.073	-0.611	
	RHA	-0.028	0.022	-0.155	-0.068	0.051	
	W	1.339	0.016	1.410	0.241	0.652	
	PL	1.237	0.206	2.035	0.116	0.305	
	FAg	-0.774	0.229	-0.960	0.045	-0.912	
		Hidden Layer 1					
		H(1:1)	**H(1:2)**	**H(1:3)**	**H(1:4)**	**H(1:5)**	**(Bias)**
Output Layer	Fc	-0.691	1.410	1.082	2.640	-0.501	-1.945

3.2.2. GP Prediction

The developed GP model has six levels of complexity. The population size, survivor size and number of generations were 200 000, 30 000 and 300 respectively. Equation 1 present the output formulas for Fc. The average error of total dataset is 13.8MPa, while the R^2 value is 0.818. The close-form equation shows the possible application of the GP model in the manual and computer computation of the compressive strength of the lightweight concrete during design and the concrete mechanical strength behavior during use.

$$\mathrm{Fc} = \frac{W.(2A-1)(C+2A)+26(A.FAg+W.PL)}{26\ W.A} + \frac{52\ A.PL.FAg^2}{W.(C+2A)(FAg+2\ A.W-W)} - \mathrm{Ln}\left(\frac{C+2A}{26\ A}\right) \tag{1}$$

3.2.3. EPR Prediction

Finally, the developed EPR model was limited to cubic level for (Fc), for 6 inputs, there are 84 possible terms (56+21+6+1=84) as follows:

$$\sum_{i=1}^{i=6}\sum_{j=1}^{j=6}\sum_{k=1}^{k=6} X_i.X_j.X_k + \sum_{i=1}^{i=6}\sum_{j=1}^{j=6} X_i.X_j + \sum_{i=1}^{i=6} X_i + C \tag{2}$$

GA technique was applied on these polynomials to select the most effective 32 terms. The outputs are illustrated in Equation 3. The average error and R^2 values were 7.9MPa and 0.951 respectively. This outcome compares well with and better than the outcome of RFR model of a previous study [60] which showed an R^2 of 0.91.

$$Fc=\frac{A.PL.FAg}{190370}+\frac{216\,A}{FAg}+\frac{16.47\,FAg}{A.W}-\frac{1.05E+08}{A.W.FAg}.-\frac{406\,PL}{A}+\frac{PL.FAg}{7.67\,A}+\frac{PL}{3.15\,A.FAg}-\frac{PL^2}{4.65\,A}+\frac{FAg}{7.45\,A}-\frac{FAg^2}{10650\,A}+\frac{3.5}{A.FAg}+\frac{C.W}{91}-\frac{C.W.PL}{537}-\frac{C.W.FAg}{75690}-\frac{7.86\,C.W}{FAg}+\frac{C.W^2}{19080}-\frac{1460\,C}{W}-\frac{56.64\,C.PL}{W}+\frac{C.FAg}{2.15W}+\frac{1.41E+06\,C}{W.FAg}+\frac{C.PL.FAg}{45750}+\frac{34.33C.PL}{FAg}+\frac{C.PL^2}{382}+\frac{C.FAg}{557.6}-\frac{C.FAg^2}{2020000}-\frac{5326.5C}{FAg}+\frac{C^2}{56}-\frac{C^2.W}{21625}-\frac{172C^2}{W}+0.59\,C.PL+1.91C+14.6 \quad (3)$$

3.2.4. GMDH-Combinatorial Prediction

The combinatorial group method of data handling algorithm (GMDH-Combi) is a single-layer parametric algorithm that is self-organizing and can carry out a full exploration of all possible models [69]. In the GMDH-Combi method, models are generated from all probable combinations of input variables, and the best final model would be chosen according to a selection criterion, which is usually an error criterion such as root mean squared error (RMSE).

The value of the single-layer self-organizing algorithms comprises straightforwardness and their ability to categorize model structure [70, 71]. It should be noted that in the GMDH-Combi approach, different combinations of input variable with user-defined-power-orders is considered and apparently a time-consuming calculation process would be formed [71-73]. For instance, considering to model a dataset with two inputs, (x1 and x2) and a target variable (y), a function of quadratic polynomial that the optimization process needs to be performed would be as $y=c0+c1\bullet x1+c2\bullet x2+c3\bullet x1\bullet x2+c4\bullet x1^2+c5\bullet x2^2$ (where ci, i = 0, 1, …, n is the model constants). GMDH-Combi would lead to choose an optimized and compound model in which $y=c0+c3\bullet x1\bullet x2$ is a subdivision of searching relationships. The aim would be finding as smallest as possible model in terms and error. As full combinatorial exploration of model with entire terms takes too much time, the search domain is limited to n terms and the user controls the number of terms in the polynomial. Many trial and error were conducted in the present database to achieve the best orders along with the least error and the best robustness. This process gave rise to the closed-form equation in Equation 4 with a performance index of 0.899 for the R^2 and 9.39% as the MAPE. This shows that GMDH-Combi performed better than GP.

$$Fc=10.5514+33.87\frac{A}{W}-\frac{127.9}{A}+\frac{0.488W}{A}+0.00004C\cdot FAg+0.013RHA\cdot PL-0.443W\cdot PL+10.8PL \quad (4)$$

Overall, Table 7 shows the summary of the performance accuracy of the models predicted by using ANN (-BP, -GRG and –GA), GP and EPR and GMDH-Combi. In Figures 9 to12, the Taylor diagram, variance diagram, best fir scatter diagram and residual sketch, respectively, which shows the standard deviation and root mean square errors comparison of the models with respect to measured data and comparison between the models and the measured data and the plot of the residuals. Although, the prediction accuracy of EPR model is lower than ANN models, but the output is a closed form equation, which could be used manually or as software unlike the ANN output which can't be used manually. The results indicated that the accuracy of the ANN model is slightly affected by the training algorithm. The back-propagation (BP) showed the best level of accuracy (94.7%), gradually reduced gradient (GRG) came in the second order with accuracy of 97.9% and genetic algorithm (GA) showed the lower level of accuracy (96%).

Table 7. Accuracies of developed models

	GP	ANN-BP	ANN-GRG	ANN-GA	EPR	GMDH-Combi
R	0.927	0.989	0.987	0.980	0.976	0.948
R^2	0.860	0.979	0.974	0.960	0.953	0.899
MSE	1893.9	2252.6	2219.9	2164.4	2102.5	1935.0
RMSE (MPa)	43.52	47.46	47.12	46.52	45.85	43.99
MAPE (%)	12.15	4.95	5.35	6.67	6.81	9.39

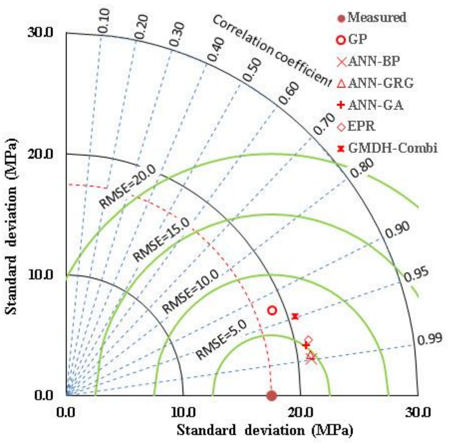

Figure 9. Comparison between developed models using Taylor diagram

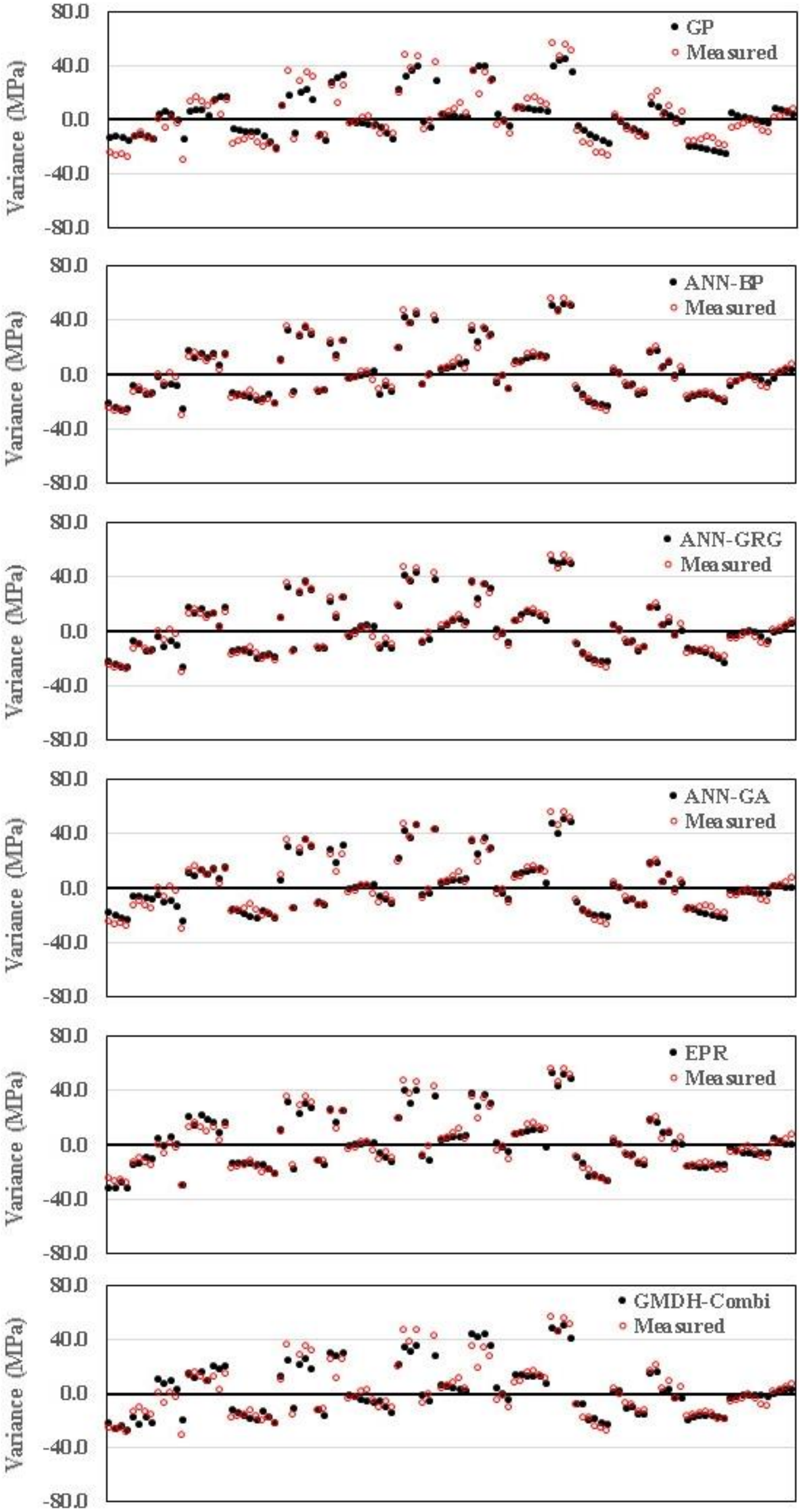

Figure 10. Comparison between developed models for (Fc) using Variance diagrams

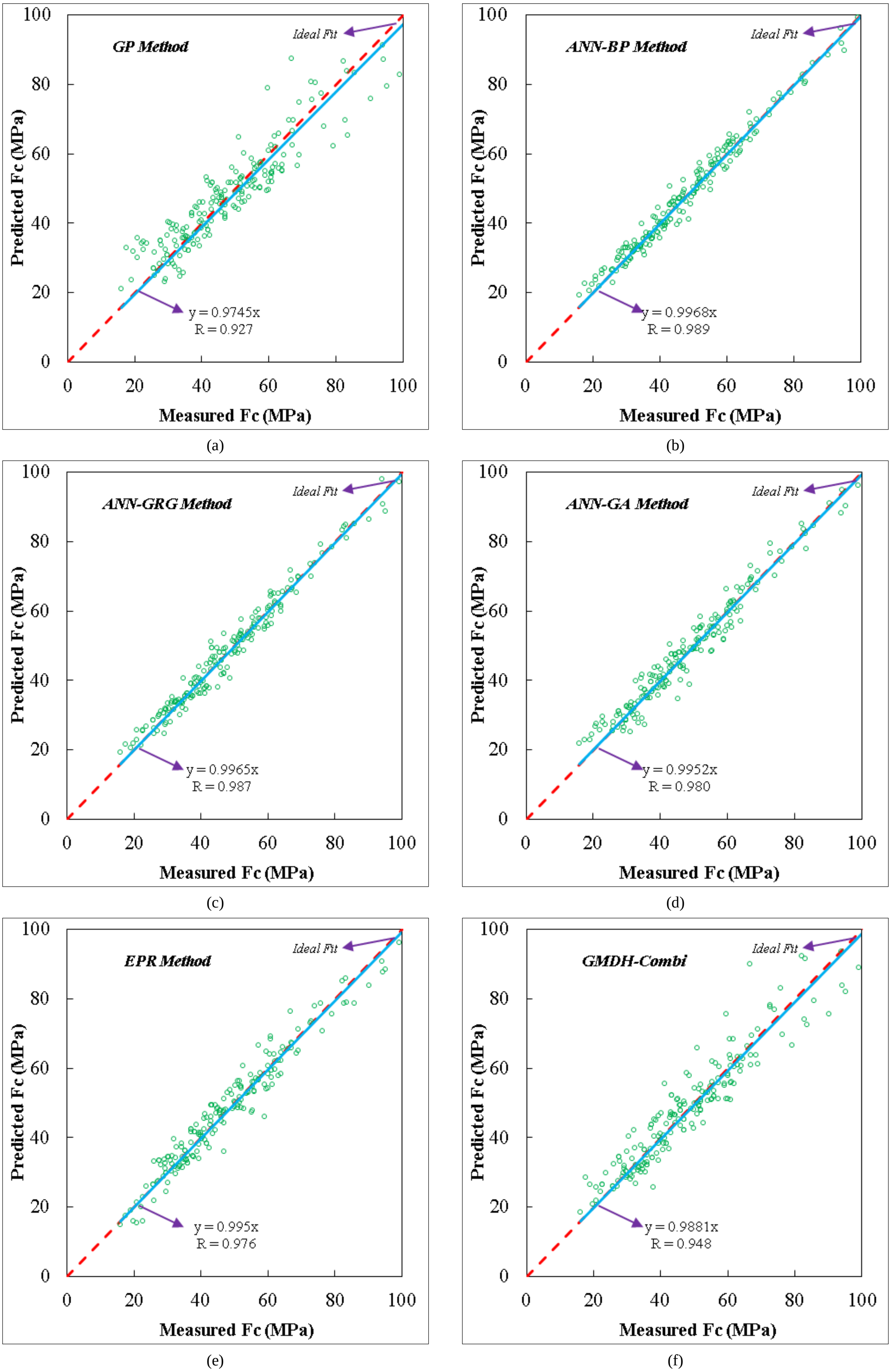

Figure 11. Relation between predicted and measured (Fc) values using the developed models; (a) GP, (b) ANN-BP, (c) ANN-GRG, (d) ANN-GA, (e) EPR, and (f) GMDH-Combi

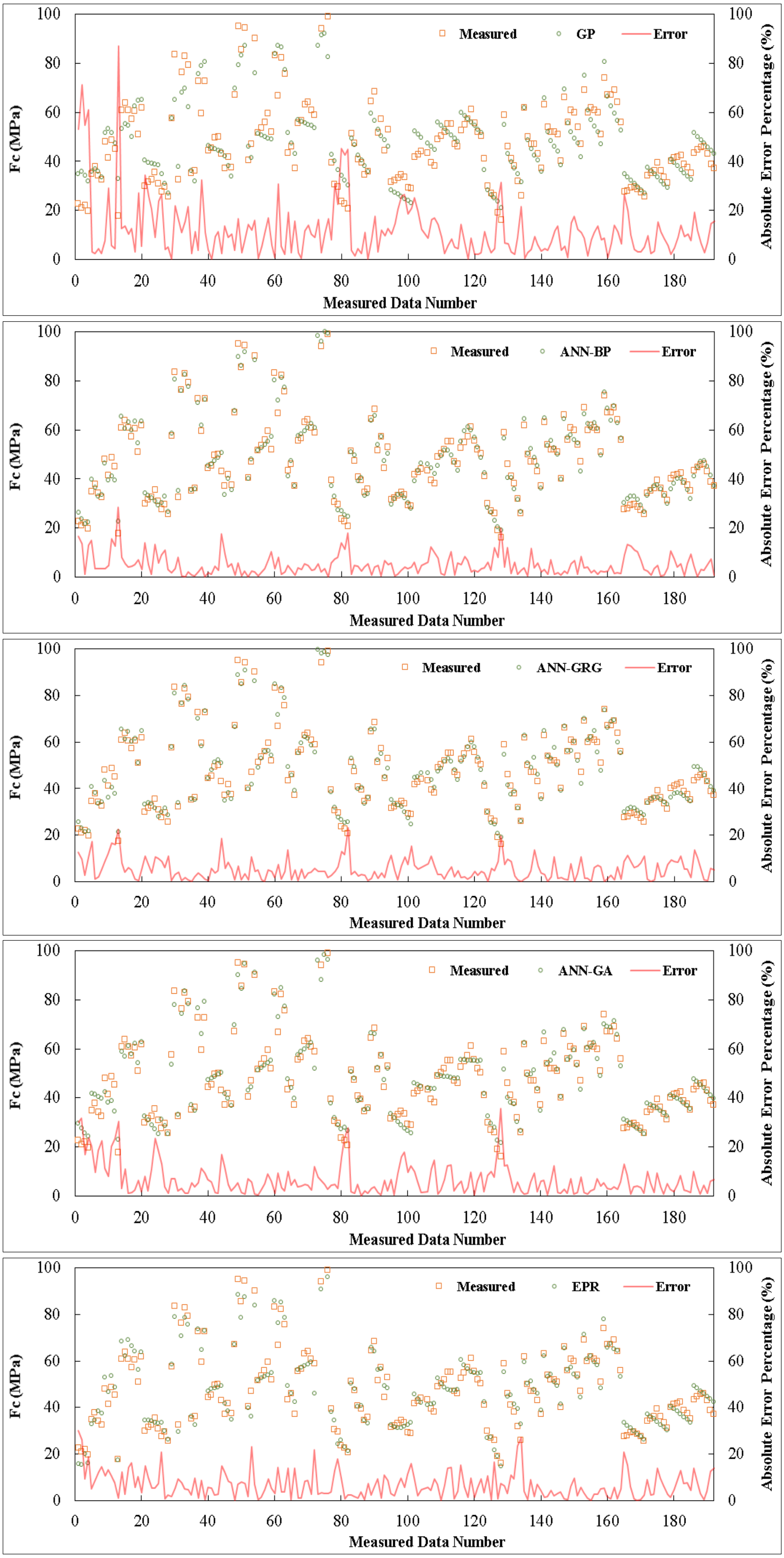
Measured
GP
Error
Fc (MPa)
Absolute Error Percentage (%)
Measured Data Number
Measured
ANN-BP
Error
Fc (MPa)
Absolute Error Percentage (%)
Measured Data Number
Measured
ANN-GRG
Error
Fc (MPa)
Absolute Error Percentage (%)
Measured Data Number
Measured
ANN-GA
Error
Fc (MPa)
Absolute Error Percentage (%)
Measured Data Number
Measured
EPR
Error
Fc (MPa)
Absolute Error Percentage (%)
Measured Data Number

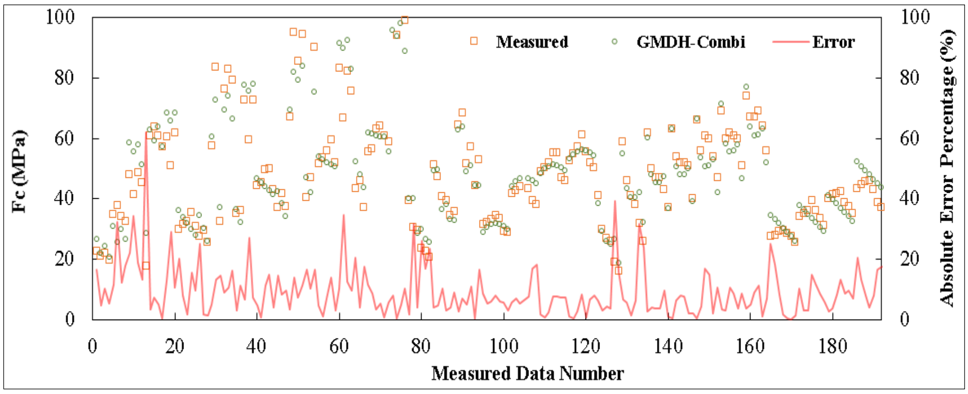

Figure 12. Comparison between the models and the measured data and the plot of the residuals

3.3. Sensitivity Analysis of the Studied UHPLC Constituents

A useful concept is provided to identify the importance of each of the "*cause*" (input) factors on the "*impact factor*" (output). This allows us to identify the most sensitive factors affecting Fc hierarchically. To achieve this goal, sensitivity analysis was performed to identify the relative impact of each parameter on output in the mode using the cosine domain method [74]. To apply this method, all of the data pairs were expressed in common X-space. To undertake this technique, all data pairs should be utilized to build a data array X as follows [75-78]:

$$X = \{x_1, x_2, x_3, \dots, x_i, \dots, x_n\} \tag{5}$$

Each of the elements, xi, in the data array X is a vector of lengths of m, that is:

$$X = \{x_1 1, x_2 2, x_3 3, \dots, x_{im}\} \tag{6}$$

The strength of the relation between the dataset, xi and xj, is presented as follows:

$$r_{ij} = \frac{\sum_{k=1}^{m} x_{ik} x_{jk}}{\sqrt{\sum_{k=1}^{m} x_{ik}^2 \sum_{k=1}^{m} x_{ik}^2}} \tag{7}$$

Results from the sensitivity analysis are shown in Figure 13. This figure shows that the PL, C, FA, W and A are the most significant parameters determining the Fc, respectively. Besides, RHA has the least effect on Fc.

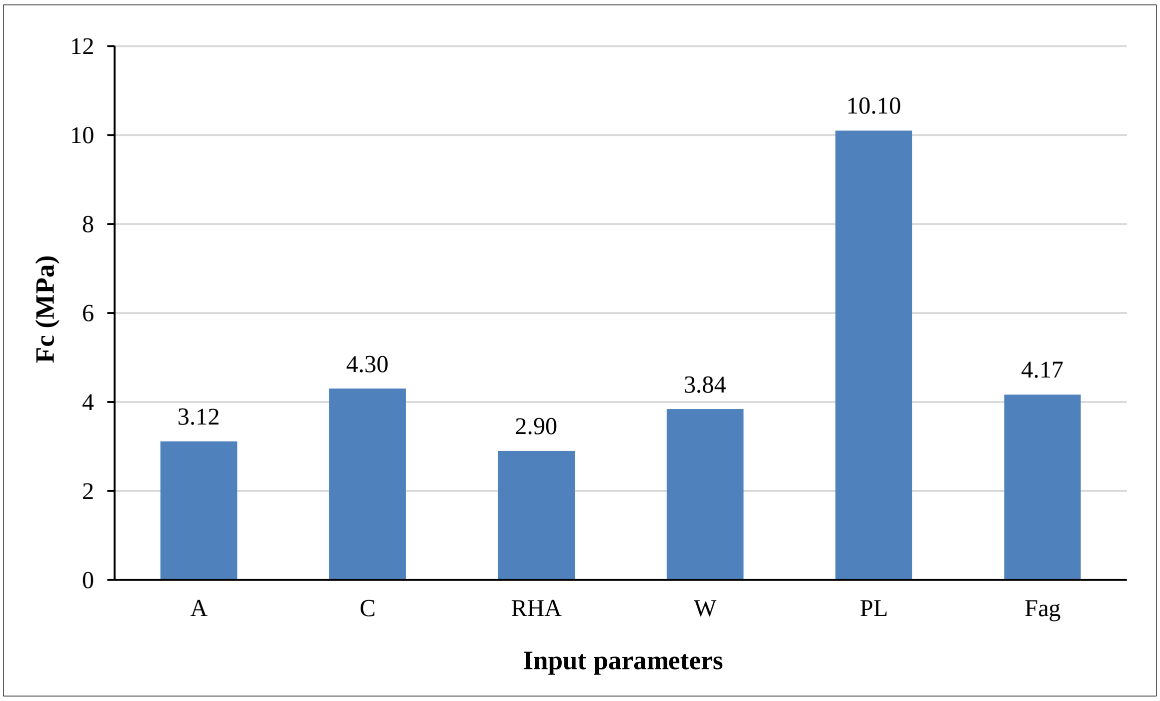

Figure 13. Sensitivity analysis to determine the impact of each data on the output

4. Conclusions

The life cycle assessment was applied to several concrete mixes incorporating OPC, rice husk ash, fine aggregates, and superplasticizer. The environmental performance of the mixtures was related mostly to the percentage of cement in the mix. Thus, the concrete structure with the highest score in the environmental performance evaluation was C-783. In contrast, C-300 was selected as the optimal choice because of the good environmental profile found in the LCA and the compressive strength associated with the concrete mix.

This research presents six models using (AI) techniques (GP, ANN-BP, ANN-GRG, ANN-GA, EPR, and GMDH-Combi) to predict the compressive strength of ultra-high-performance concrete at a certain age (Fc) using concrete age (A), cement content (C), rice husk ash content (RHA), water content (W), super plasticizer content (PL), and fine aggregate content (FAg). The results of comparing the accuracies of the developed models could be concluded in the following points:

- GP model is the simplest and the less accurate one (86.0%). Then EPR and ANN-GA with accuracy of 95.3% and 96% respectively, finally ANN-BP and ANN-GRG models have almost the same accuracy of 97.9% and 97.4%, respectively while the GMDH-Combi has a performance of 89.9%;
- The sensitivity analysis of the variables indicates that the plasticizer (PL) is the most important factor, then cement and fine aggregates, while rice husk ash is the least influential;
- Both the GP and EPR models didn't include RHA, which indicated its minor impact on the concrete strength. However, GMDH-Combi showed better performance than GP and had a less complex closed-form equation;
- The GA technique successfully reduced the 84 terms of the conventional polynomial regression quadrilateral formula to only 32 terms without significant impact on its accuracy;
- The GA technique successfully reduced the 84 terms of the conventional polynomial regression quadrilateral formula to only 32 terms without significant impact on its accuracy.

5. Declarations

5.1. Author Contributions

Conceptualization, K.C.O.; methodology, A.M.E.; software, A.R.; formal analysis, D.R.E.; investigation, H.B.; visualization, A.S., editing, D.N.K.; statistical analysis, J.S.; modeling, H.J., supervision, H.A.M. All authors have read and agreed to the published version of the manuscript.

5.2. Data Availability Statement

The data presented in this study are available in the article.

5.3. Funding

The authors received no financial support for the research, authorship, and/or publication of this article.

5.4. Conflicts of Interest

The authors declare no conflict of interest.

6. References

[1] Ingrao, C., Scrucca, F., Tricase, C., & Asdrubali, F. (2016). A comparative Life Cycle Assessment of external wall-compositions for cleaner construction solutions in buildings. Journal of Cleaner Production, 124, 283–298. doi:10.1016/j.jclepro.2016.02.112.

[2] Soleimani, T., Hayek, M., Junqua, G., Salgues, M., & Souche, J. C. (2022). Environmental, economic and experimental assessment of the valorization of dredged sediment through sand substitution in concrete. Science of the Total Environment, 159980. doi:10.1016/j.scitotenv.2022.159980.

[3] Colangelo, F., Forcina, A., Farina, I., & Petrillo, A. (2018). Life Cycle Assessment (LCA) of different kinds of concrete containing waste for sustainable construction. Buildings, 8(5), 70. doi:10.3390/buildings8050070.

[4] Soleymani, A., & Esfahani, mohammad R. (2019). Effect of concrete strength and thickness of flat slab on preventing of progressive collapse caused by elimination of an internal column. Journal of Structural and Construction Engineering, 6(1), 24–40. doi:10.22065/jsce.2017.98444.1335.

[5] Rodríguez, G., Medina, C., Alegre, F. J., Asensio, E., & De Sánchez Rojas, M. I. (2015). Assessment of Construction and Demolition Waste plant management in Spain: In pursuit of sustainability and eco-efficiency. Journal of Cleaner Production, 90, 16–24. doi:10.1016/j.jclepro.2014.11.067.

[6] Caldas, L., Martins, M., Lima, D., & Sposto, R. (2016). Literature review of life cycle assessment applied to green concretes. Proceedings of the 6th Amazon & Pacific Green Materials Congress and Sustainable Construction Materials Lat-Rilem Conference, 27-29 April, 2016, Cali, Colombia.

[7] Surahman, U., Kubota, T., & Higashi, O. (2015). Life cycle assessment of energy and CO2 emissions for residential buildings in Jakarta and Bandung, Indonesia. Buildings, 5(4), 1131–1155. doi:10.3390/buildings5041131.

[8] Peng, K., Wu, L., Zandi, Y., Agdas, A. S., Majdi, A., Denic, N., Zakić, A., Khalek Ebid, A. A., Khadimallah, M. A., & Ali, H. E. (2022). Application of Polyacrylic Hydrogel in Durability and Reduction of Environmental Impacts of Concrete through ANN. Gels, 8(8), 468. doi:10.3390/gels8080468.

[9] Alyousef, R., Mohammadhosseini, H., Ebid, A. A. K., Alabduljabbar, H., Ngian, S. P., & Mohamed, A. M. (2022). Durability Enhancement of Sustainable Concrete Composites Comprising Waste Metalized Film Food Packaging Fibers and Palm Oil Fuel Ash. Sustainability (Switzerland), 14(9), 5253. doi:10.3390/su14095253.

[10] Min, J., Zandi, Y., Agdas, A. S., Majdi, A., Ali, H. E., Jan, A., Salameh, A. A., & Ebid, A. A. K. (2022). The Numerical Analysis of Replenishment of Hydrogel Void Space Concrete Using Hydrogels Containing Nano-Silica Particles through ELM-ANFIS. Gels, 8(5), 8,299. doi:10.3390/gels8050299.

[11] Liu, Q., Peng, K., Zandi, Y., Agdas, A. S., Al-Tamimi, H. M., Assilzadeh, H., Khalek Ebid, A. A., Khadimallah, M. A., & Ali, H. E. (2022). Mechanical Characteristics and Self-Healing Soil-Cementitious Hydrogel Materials in Mine Backfill Using Hybridized ANFIS-SVM. Gels, 8(7), 455. doi:10.3390/gels8070455.

[12] Reddy, S. V. B., & Srinivasa Rao, P. (2020). Experimental studies on mechanical properties and impact characteristics of ternary concrete with steel fiber. Materials Today: Proceedings, 27, 788–797. doi:10.1016/j.matpr.2019.12.344.

[13] Iswarya, G., & Beulah, M. (2021). Use of zeolite and industrial waste materials in high strength concrete - A review. Materials Today: Proceedings, 46, 116–123. doi:10.1016/j.matpr.2020.06.329.

[14] Shen, L., Li, Q., Ge, W., & Xu, S. (2020). The mechanical property and frost resistance of roller compacted concrete by mixing silica fume and limestone powder: Experimental study. Construction and Building Materials, 239, 117882. doi:10.1016/j.conbuildmat.2019.117882.

[15] Habeeb, G. A., Mahmud, H. B., & Hamid, N. B. A. A. (2010). Assessment of deterioration in RHA-concrete due to magnesium sulphate attack. International Journal of Minerals, Metallurgy and Materials, 17(6), 691–696. doi:10.1007/s12613-010-0375-8.

[16] Manjunatha, M., Vijaya Bhaskar Raju, K., Sivapullaiah, P.V. (2021). Effect of PVC Dust on the Performance of Cement Concrete—A Sustainable Approach. Recent Developments in Sustainable Infrastructure. Lecture Notes in Civil Engineering, 75. Springer, Singapore. doi:10.1007/978-981-15-4577-1_52.

[17] Mohan, A., & Mini, K. M. (2018). Strength Studies of SCC Incorporating Silica Fume and Ultra-Fine GGBS. Materials Today: Proceedings, 5(11), 23752–23758. doi:10.1016/j.matpr.2018.10.166.

[18] Jincheng, X., Weichang, H., Xinli, K., & Tianmin, W. (2001). Research and development of the object-oriented life cycle assessment database. Materials and Design, 22(2), 101–105. doi:10.1016/s0261-3069(00)00049-2.

[19] Xiao, D., Wang, H., Zhu, J., & Peng, S. (2001). Sequent and accumulative life cycle assessment of materials and products. Materials and Design, 22(2), 147–149. doi:10.1016/S0261-3069(00)00057-1.

[20] Finnveden, G., Hauschild, M. Z., Ekvall, T., Guinée, J., Heijungs, R., Hellweg, S., Koehler, A., Pennington, D., & Suh, S. (2009). Recent developments in Life Cycle Assessment. Journal of Environmental Management, 91(1), 1–21. doi:10.1016/j.jenvman.2009.06.018.

[21] Finkbeiner, M., Inaba, A., Tan, R. B. H., Christiansen, K., & Klüppel, H. J. (2006). The new international standards for life cycle assessment: ISO 14040 and ISO 14044. International Journal of Life Cycle Assessment, 11(2), 80–85. doi:10.1065/lca2006.02.002.

[22] Estanqueiro, B., Dinis Silvestre, J., de Brito, J., & Duarte Pinheiro, M. (2018). Environmental life cycle assessment of coarse natural and recycled aggregates for concrete. European Journal of Environmental and Civil Engineering, 22(4), 429–449. doi:10.1080/19648189.2016.1197161.

[23] Turk, J., Cotič, Z., Mladenovič, A., & Šajna, A. (2015). Environmental evaluation of green concretes versus conventional concrete by means of LCA. Waste Management, 45, 194–205. doi:10.1016/j.wasman.2015.06.035.

[24] Kleijer, A. L., Lasvaux, S., Citherlet, S., & Viviani, M. (2017). Product-specific Life Cycle Assessment of ready mix concrete: Comparison between a recycled and an ordinary concrete. Resources, Conservation and Recycling, 122, 210–218. doi:10.1016/j.resconrec.2017.02.004.

[25] Colangelo, F., Petrillo, A., Cioffi, R., Borrelli, C., & Forcina, A. (2018). Life cycle assessment of recycled concretes: A case study in southern Italy. Science of the Total Environment, 615, 1506–1517. doi:10.1016/j.scitotenv.2017.09.107.

[26] Colangelo, F., & Cioffi, R. (2017). Mechanical properties and durability of mortar containing fine fraction of demolition wastes produced by selective demolition in South Italy. Composites Part B: Engineering, 115, 43–50. doi:10.1016/j.compositesb.2016.10.045.

[27] Vieira, D. R., Calmon, J. L., & Coelho, F. Z. (2016). Life cycle assessment (LCA) applied to the manufacturing of common and ecological concrete: A review. Construction and Building Materials, 124, 656–666. doi:10.1016/j.conbuildmat.2016.07.125.

[28] Schmidt, M., & Fehling, E. (2005). Ultra-high-performance concrete: research, development and application in Europe. ACI Spec. Publ, 228(1), 51-78.

[29] Graybeal, B. (2011). Ultra-high-performance concrete. No. FHWA-HRT-11-038, Federal Highway Administration, Washington, United States.

[30] Meng, W., Valipour, M., & Khayat, K. H. (2017). Optimization and performance of cost-effective ultra-high-performance concrete. Materials and Structures/Materiaux et Constructions, 50(1), 29. doi:10.1617/s11527-016-0896-3.

[31] Jamil, M., Kaish, A. B. M. A., Raman, S. N., & Zain, M. F. M. (2013). Pozzolanic contribution of rice husk ash in cementitious system. Construction and Building Materials, 47, 588–593. doi:10.1016/j.conbuildmat.2013.05.088.

[32] Nair, D. G., Fraaij, A., Klaassen, A. A. K., & Kentgens, A. P. M. (2008). A structural investigation relating to the pozzolanic activity of rice husk ashes. Cement and Concrete Research, 38(6), 861–869. doi:10.1016/j.cemconres.2007.10.004.

[33] Salas, A., Delvasto, S., de Gutierrez, R. M., & Lange, D. (2009). Comparison of two processes for treating rice husk ash for use in high performance concrete. Cement and Concrete Research, 39(9), 773–778. doi:10.1016/j.cemconres.2009.05.006.

[34] Chao-Lung, H., Anh-Tuan, B. Le, & Chun-Tsun, C. (2011). Effect of rice husk ash on the strength and durability characteristics of concrete. Construction and Building Materials, 25(9), 3768–3772. doi:10.1016/j.conbuildmat.2011.04.009.

[35] Chandrasekhar, S., Satyanarayana, K. G., Pramada, P. N., Raghavan, P., & Gupta, T. N. (2003). Processing, properties and applications of reactive silica from rice husk - An overview. Journal of Materials Science, 38(15), 3159–3168. doi:10.1023/A:1025157114800.

[36] Babu, T. R., & Neeraja, D. (2016). Rice husk ash as supplementary material in concrete–A review. International Journal of chemTech Research, 9(5), 332-337.

[37] Abuhaikal, M. M. A. (2011). Nano-chemomechanical assessment of rice husk ash cement by wavelength dispersive spectroscopy and nanoindentation. PhD Thesis, Massachusetts Institute of Technology, Massachusetts, United States.

[38] Bobkowski, B. (2015). Performance of ternary cementitious binder systems incorporating untreated and treated pozzolanic materials. Knowledge Exchange for Young Scientists (KEYS), 9th – 11th June 2015, Dar es Salaam, Tanzania.

[39] Rodríguez De Sensale, G. (2010). Effect of rice-husk ash on durability of cementitious materials. Cement and Concrete Composites, 32(9), 718–725. doi:10.1016/j.cemconcomp.2010.07.008.

[40] Khan, M. I., & Alhozaimy, A. M. (2011). Properties of natural pozzolan and its potential utilization in environmental friendly concrete. Canadian Journal of Civil Engineering, 38(1), 71–78. doi:10.1139/L10-112.

[41] Zhang, M. H., Lastra, R., & Malhotra, V. M. (1996). Rice-husk ash paste and concrete: Some aspects of hydration and the microstructure of the interfacial zone between the aggregate and paste. Cement and Concrete Research, 26(6), 963–977. doi:10.1016/0008-8846(96)00061-0.

[42] Givi, A. N., Rashid, S. A., Aziz, F. N. A., & Salleh, M. A. M. (2010). Assessment of the effects of rice husk ash particle size on strength, water permeability and workability of binary blended concrete. Construction and Building Materials, 24(11), 2145–2150. doi:10.1016/j.conbuildmat.2010.04.045.

[43] Kang, S. H., Hong, S. G., & Moon, J. (2019). The use of rice husk ash as reactive filler in ultra-high performance concrete. Cement and Concrete Research, 115, 389–400. doi:10.1016/j.cemconres.2018.09.004.

[44] Hossain, S. S., & Roy, P. K. (2020). Waste rice husk ash derived sol: A potential binder in high alumina refractory castables as a replacement of hydraulic binder. Journal of Alloys and Compounds, 817, 152806. doi:10.1016/j.jallcom.2019.152806.

[45] Mohseni, E., Kazemi, M. J., Koushkbaghi, M., Zehtab, B., & Behforouz, B. (2019). Evaluation of mechanical and durability properties of fiber-reinforced lightweight geopolymer composites based on rice husk ash and nano-alumina. Construction and Building Materials, 209, 532–540. doi:10.1016/j.conbuildmat.2019.03.067.

[46] Boontawee, K., Pansuk, W., Tachai, L., & Kondoh, K. (2018). Effect of Rice Husk Ash Silica as Cement Replacement for Making Construction Mortar. Key Engineering Materials, 775, 624–629. doi:10.4028/www.scientific.net/kem.775.624.

[47] Huang, H., Gao, X., Wang, H., & Ye, H. (2017). Influence of rice husk ash on strength and permeability of ultra-high-performance concrete. Construction and Building Materials, 149, 621–628. doi:10.1016/j.conbuildmat.2017.05.155.

[48] Miyandehi, B. M., Feizbakhsh, A., Yazdi, M. A., Liu, Q. feng, Yang, J., & Alipour, P. (2016). Performance and properties of mortar mixed with nano-CuO and rice husk ash. Cement and Concrete Composites, 74, 225–235. doi:10.1016/j.cemconcomp.2016.10.006.

[49] Jahangir, H., & Esfahani, M. R. (2020). Investigating loading rate and fibre densities influence on SRG - concrete bond behaviour. Steel and Composite Structures, 34(6), 877–889. doi:10.12989/scs.2020.34.6.877.

[50] Agwa, I. S., Omar, O. M., Tayeh, B. A., & Abdelsalam, B. A. (2020). Effects of using rice straw and cotton stalk ashes on the properties of lightweight self-compacting concrete. Construction and Building Materials, 235, 117541. doi:10.1016/j.conbuildmat.2019.117541.

[51] Jahangir, H., & Esfahani, M. R. (2022). Bond Behavior Investigation between steel reinforced grout composites and masonry substrate. Iranian Journal of Science and Technology - Transactions of Civil Engineering, 46(5), 3519–3535. doi:10.1007/s40996-022-00826-9.

[52] Wang, W., Meng, Y., & Wang, D. (2017). Effect of Rice Husk Ash on High-Temperature Mechanical Properties and Microstructure of Concrete. Kemija u Industriji, 66(3–4), 157–164. doi:10.15255/kui.2016.054.

[53] Van Tuan, N., Ye, G., Van Breugel, K., Fraaij, A. L. A., & Bui, D. D. (2011). The study of using rice husk ash to produce ultra-high performance concrete. Construction and Building Materials, 25(4), 2030–2035. doi:10.1016/j.conbuildmat.2010.11.046.

[54] Lu, J. X., Shen, P., Ali, H. A., & Poon, C. S. (2022). Mix design and performance of lightweight ultra-high-performance concrete. Materials and Design, 216, 110553. doi:10.1016/j.matdes.2022.110553.

[55] Van Den Heede, P., & De Belie, N. (2012). Environmental impact and life cycle assessment (LCA) of traditional and "green" concretes: Literature review and theoretical calculations. Cement and Concrete Composites, 34(4), 431–442. doi:10.1016/j.cemconcomp.2012.01.004.

[56] Liu, C., Ahn, C. R., An, X., & Lee, S. (2013). Life-Cycle Assessment of Concrete Dam Construction: Comparison of Environmental Impact of Rock-Filled and Conventional Concrete. Journal of Construction Engineering and Management, 139(12), 4013009. doi:10.1061/(asce)co.1943-7862.0000752.

[57] Tait, M. W., & Cheung, W. M. (2016). A comparative cradle-to-gate life cycle assessment of three concrete mix designs. International Journal of Life Cycle Assessment, 21(6), 847–860. doi:10.1007/s11367-016-1045-5.

[58] Anastasiou, E. K., Liapis, A., & Papayianni, I. (2015). Comparative life cycle assessment of concrete road pavements using industrial by-products as alternative materials. Resources, Conservation and Recycling, 101, 1–8. doi:10.1016/j.resconrec.2015.05.009.

[59] Kurad, R., Silvestre, J. D., de Brito, J., & Ahmed, H. (2017). Effect of incorporation of high volume of recycled concrete aggregates and fly ash on the strength and global warming potential of concrete. Journal of Cleaner Production, 166, 485–502. doi:10.1016/j.jclepro.2017.07.236.

[60] Iftikhar, B., Alih, S. C., Vafaei, M., Elkotb, M. A., Shutaywi, M., Javed, M. F., Deebani, W., Khan, M. I., & Aslam, F. (2022). Predictive modeling of compressive strength of sustainable rice husk ash concrete: Ensemble learner optimization and comparison. Journal of Cleaner Production, 348, 131285. doi:10.1016/j.jclepro.2022.131285.

[61] ISO 14040:2006 (2006). Environmental management-Life cycle assessment-Principles and framework. International Organization for Standardization (ISO), Geneva, Switzerland.

[62] Wernet, G., Bauer, C., Steubing, B., Reinhard, J., Moreno-Ruiz, E., & Weidema, B. (2016). The Eco invent database version 3 (part I): overview and methodology. International Journal of Life Cycle Assessment, 21(9), 1218–1230. doi:10.1007/s11367-016-1087-8.

[63] Huijbregts, M. A. J., Steinmann, Z. J. N., Elshout, P. M. F., Stam, G., Verones, F., Vieira, M., Zijp, M., Hollander, A., & van Zelm, R. (2017). ReCiPe2016: a harmonised life cycle impact assessment method at midpoint and endpoint level. International Journal of Life Cycle Assessment, 22(2), 138–147. doi:10.1007/s11367-016-1246-y.

[64] Asadollahfardi, G., Katebi, A., Taherian, P., & Panahandeh, A. (2021). Environmental life cycle assessment of concrete with different mixed designs. International Journal of Construction Management, 21(7), 665–676. doi:10.1080/15623599.2019.1579015.

[65] Pillai, R. G., Gettu, R., Santhanam, M., Rengaraju, S., Dhandapani, Y., Rathnarajan, S., & Basavaraj, A. S. (2019). Service life and life cycle assessment of reinforced concrete systems with limestone calcined clay cement (LC3). Cement and Concrete Research, 118, 111–119. doi:10.1016/j.cemconres.2018.11.019.

[66] Sjunnesson, J. (2005). Life Cycle Assessment of Concrete. Master Thesis, Department of Technology and Society, Lund University, Lund, Sweden.

[67] Kurda, R., Silvestre, J. D., & de Brito, J. (2018). Life cycle assessment of concrete made with high volume of recycled concrete aggregates and fly ash. Resources, Conservation and Recycling, 139, 407–417. doi:10.1016/j.resconrec.2018.07.004.

[68] Garcia-Troncoso, N., Baykara, H., Cornejo, M. H., Riofrio, A., Tinoco-Hidalgo, M., & Flores-Rada, J. (2022). Comparative mechanical properties of conventional concrete mixture and concrete incorporating mining tailings sands. Case Studies in Construction Materials, 16, 1031. doi:10.1016/j.cscm.2022.e01031.

[69] Anastasakis, L., & Mort, N. (2001). The development of self-organization techniques in modelling: a review of the group method of data handling (GMDH). Research Report, Department of Automatic Control and Systems Engineering, University of Sheffield, Sheffield, United Kingdom.

[70] Ivakhnenko, A. G., Krotov, G. I., & Stepashko, V. (1983). Harmonic and Exponential Harmonic Gmdh Algorithms. Part 2. Multilayer Algorithms With and Without Calculation of Remainders. Soviet Automatic Control, 16(1), 1–9.

[71] Naderpour, H., Rezazadeh Eidgahee, D., Fakharian, P., Rafiean, A. H., & Kalantari, S. M. (2020). A new proposed approach for moment capacity estimation of ferrocement members using Group Method of Data Handling. Engineering Science and Technology, an International Journal, 23(2), 382–391. doi:10.1016/j.jestch.2019.05.013.

[72] Rezazadeh Eidgahee, D., Jahangir, H., Solatifar, N., Fakharian, P., & Rezaeemanesh, M. (2022). Data-driven estimation models of asphalt mixtures dynamic modulus using ANN, GP and combinatorial GMDH approaches. Neural Computing and Applications, 34(20), 17289–17314. doi:10.1007/s00521-022-07382-3.

[73] Onyelowe, K. C., Kontoni, D. P. N., Ebid, A. M., Dabbaghi, F., Soleymani, A., Jahangir, H., & Nehdi, M. L. (2022). Multi-Objective Optimization of Sustainable Concrete Containing Fly Ash Based on Environmental and Mechanical Considerations. Buildings, 12(7), 948. doi:10.3390/buildings12070948.

[74] Yang, Y., & Zhang, Q. (1997). A hierarchical analysis for rock engineering using artificial neural networks. Rock Mechanics and Rock Engineering, 30(4), 207–222. doi:10.1007/BF01045717.

[75] Onyelowe, K. C., Shakeri, J., Amini-Khoshalan, H., Usungedo, T. F., & Alimoradi-Jazi, M. (2022). Computational Modeling of Desiccation Properties (CW, LS, and VS) of Waste-Based Activated Ash-Treated Black Cotton Soil for Sustainable Subgrade Using Artificial Neural Network, Gray-Wolf, and Moth-Flame Optimization Techniques. Advances in Materials Science and Engineering, 2022. doi:10.1155/2022/4602064.

[76] Onyelowe, K. C., Ebid, A. M., de Jesús Arrieta Baldovino, J., & Onyia, M. E. (2022). Hydraulic conductivity predictive model of RHA-ameliorated laterite for solving landfill liner leachate, soil and water contamination and carbon emission problems. International Journal of Low-Carbon Technologies. doi:10.1093/ijlct/ctac077.

[77] Shakeri, J., Khoshalan, H. A., Dehghani, H., Bascompta, M., & Onyelowe, K. (2022). Developing New Models for Flyrock Distance Assessment in Open-Pit Mines. Journal of Mining and Environment, 13(2), 377–391. doi:10.22044/jme.2022.11805.2170.

[78] Moomivand, H., Amini Khoshalan, H., Shakeri, J., & Vandyousefi, H. (2022). Development of new comprehensive relations to assess rock fragmentation by blasting for different open pit mines using GEP algorithm and MLR procedure. International Journal of Mining and Geo-Engineering. doi:10.22059/IJMGE.2022.339174.594951.